Developmental Cell
Article

Hair Follicle Dermal Stem Cells Regenerate the Dermal Sheath, Repopulate the Dermal Papilla, and Modulate Hair Type

Waleed Rahmani,[1] Sepideh Abbasi,[1] Andrew Hagner,[1] Eko Raharjo,[1] Ranjan Kumar,[4] Akitsu Hotta,[5] Scott Magness,[6] Daniel Metzger,[7] and Jeff Biernaskie[1,2,3,4,*]
[1]Department of Comparative Biology and Experimental Medicine, Faculty of Veterinary Medicine
[2]Department of Surgery, Faculty of Medicine
[3]Alberta Children's Hospital Research Institute
[4]Hotchkiss Brain Institute
University of Calgary, Calgary, AB T2N 4N1, Canada
[5]CiRA, Kyoto University, Kyoto 606-8507, Japan
[6]University of North Carolina at Chapel Hill, Chapel Hill, NC 27599, USA
[7]Institut de Génétique et de biologie Moléculaire et Cellulaire, INSERM U964, CNRS UMR 7104, Université de Strasbourg, BP 10142 Illkirch Cedex, France
*Correspondence: jeff.biernaskie@ucalgary.ca
http://dx.doi.org/10.1016/j.devcel.2014.10.022

SUMMARY

The dermal papilla (DP) provide instructive signals required to activate epithelial progenitors and initiate hair follicle regeneration. DP cell numbers fluctuate over the hair cycle, and hair loss is associated with gradual depletion/atrophy of DP cells. How DP cell numbers are maintained in healthy follicles remains unclear. We performed in vivo fate mapping of adult hair follicle dermal sheath (DS) cells to determine their lineage relationship with DP and found that a subset of DS cells are retained following each hair cycle, exhibit self-renewal, and repopulate the DS and the DP with new cells. Ablating these hair follicle dermal stem cells and their progeny retarded hair regrowth and altered hair type specification, suggesting that they function to modulate normal DP function. This work identifies a bipotent stem cell within the adult hair follicle mesenchyme and has important implications toward restoration of hair growth after injury, disease, and aging.

INTRODUCTION

The adult mammalian skin and hair follicle (HF) contain several distinct populations of stem cells that support considerable capacity for regeneration. HF regeneration is dependent on the interaction between epithelial precursors that reside in the "bulge" (Blanpain et al., 2004; Cotsarelis et al., 1990) and specialized mesenchymal cells located at the base of the follicle called the dermal papilla (DP). DP cells provide instructive signals required to induce epithelial bulge cell proliferation and consequent initiation of anagen follicle growth (Jahoda et al., 1984; Rompolas et al., 2012). Recent work has shown that DP cells also influence the proliferative behavior of epithelial matrix progenitors within the mature hair bulb, thereby indirectly modulating hair growth (Clavel et al., 2012). Interestingly, although the number of cells within the DP fluctuates over the course of the hair cycle, it is not known how these cells are maintained or replenished, particularly because cells within the DP only rarely undergo mitotic division (Tobin et al., 2003).

Based on static measurements of DP cell number and proliferation kinetics within the HF mesenchyme (Tobin et al., 2003), it has long been speculated that a distinct precursor population may exist within the surrounding dermal sheath (DS) (Jahoda, 2003), acting as a reservoir for new DP cells. Several studies have provided indirect evidence to support this. First, microdissection and transplantation of in vitro expanded whisker-derived DS cells suggested there may be functional overlap between DS and DP cell populations (McElwee et al., 2003). Second, a progressive increase in cells lacking the DP marker *Corin-cre:lacZ* (Chi et al., 2010) suggested a heterogeneous origin of DP cells. Finally, prospectively isolated *Sox2*-expressing cells exhibited self-renewal in vitro, generated multiple dermal cell types following transplant in vivo, and reconstituted both the DP and DS of newly formed HFs (Biernaskie et al., 2009). Taken together, these experiments provided indirect evidence of an adult hair follicle mesenchymal stem cell; however, definitive evidence of their location within this niche, the functional lineage relationship between mesenchymal cell compartments (i.e., DP and DS) and the signaling that regulates their behavior remains unclear.

Here, we hypothesized that the adult DS harbors a self-renewing dermal stem cell that acts to repopulate the DS and the DP of adult HFs. To test this, we utilized an inducible in vivo genetic lineage tracing strategy to examine the fate of DS cells in adult HFs. We found that the DS contains a self-renewing population of cells that are retained within this mesenchymal niche over several consecutive bouts of HF regeneration. At the onset of each anagen growth stage, these hair follicle dermal stem cells (hfDSCs) are mobilized to regenerate a new DS and supply new cells to the DP. In vivo clonal fate mapping showed that within a given hair cycle, individual hfDSCs

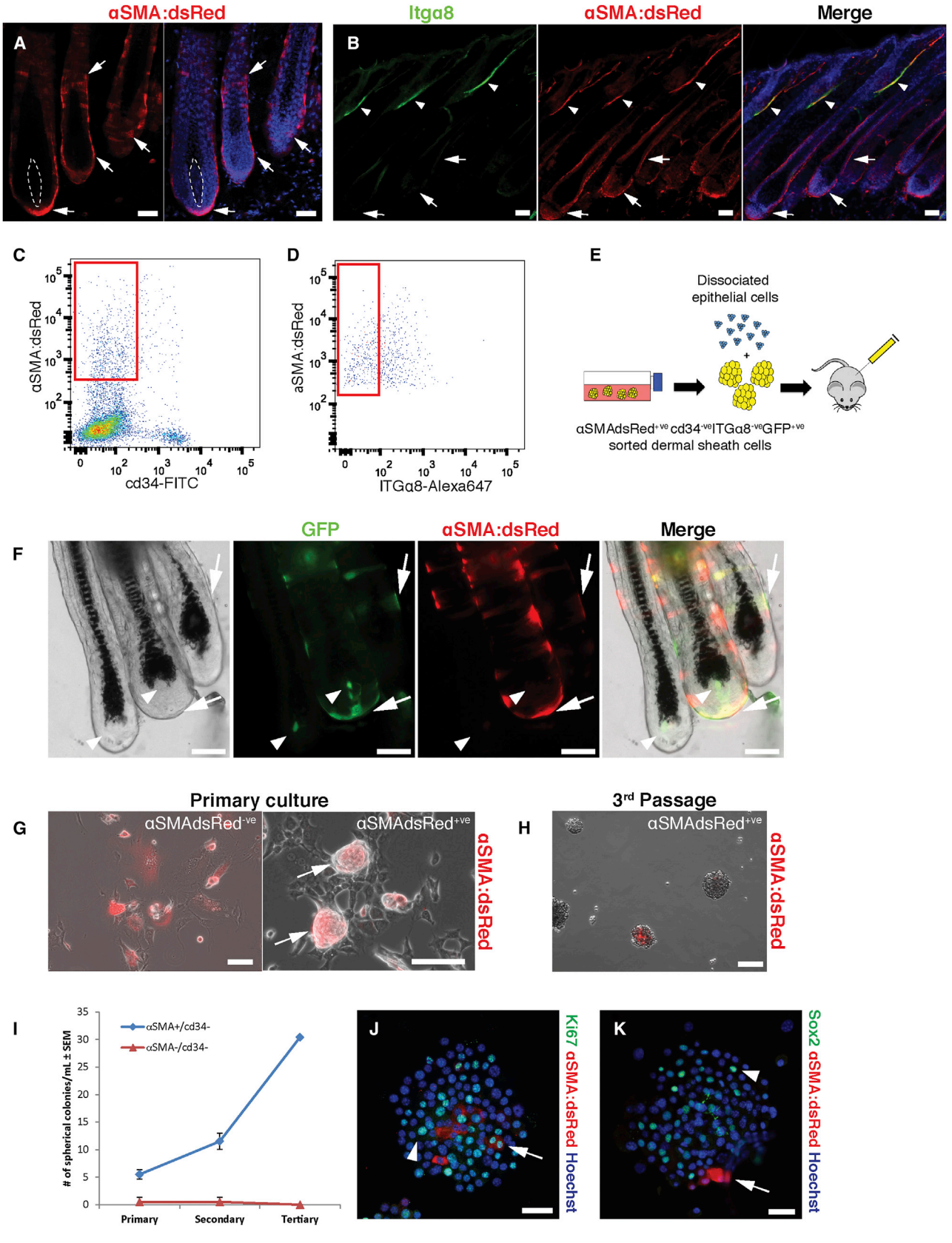

(legend on next page)

generated progeny that repopulate both DS and DP. Finally, we show that recruitment of hfDSC progeny into the DP is required to maintain normal anagen onset and to permit formation of large hair types.

RESULTS

Proliferation within the Adult Hair Follicle Mesenchyme Is Largely Restricted to the DS Compartment

In order to determine the lineage relationship between cells within the HF mesenchyme, we compared cell division within the DP and DS compartments over the course of the first adult hair cycle. Similar to previous reports (Tobin et al., 2003), quantification of Ki67 staining at various time points revealed that the HF mesenchymal cells are activated to divide at early anagen and with diminishing proliferation through mid to late anagen (Figures S1A–S1C available online). Comparison of cell proliferation within DS and DP compartments showed that mitotic activity was almost exclusively localized to cells within the DS (Figures S1B–S1D). That is, 38% of DS cells were dividing during early anagen and declined to 8.6% at mid-anagen and finally 2.1% at catagen. In contrast, 0.76% of DP cells per follicle were found to be dividing and this was only observed during early anagen stage (Figure S1D).

Prospectively Isolated DS Cells Reconstitute the Hair Follicle Mesenchyme

Based on an overall lack of proliferation in the adult DP, we surmised that the DS, and not DP, is the primary residence for a putative HF mesenchymal precursor. Our previous work showed that prospectively isolated neonatal *Sox2*-expressing SKPs (that includes both DP and DS cells) are capable of reconstituting the DS and the DP in an ex vivo HF reconstitution assay (Biernaskie et al., 2009). Therefore, we postulated that if precursors reside within the adult DS, then isolated DS cells should be capable of reconstituting both DP and DS compartments of the HF. Adult anagen DS cells can be exclusively distinguished from DP cells by their robust expression of alpha-smooth muscle actin (αSMA) (Jahoda et al., 1991). Therefore, to prospectively isolate DS cells, we took advantage of an *αSMAdsRed* knockin mouse (Magness et al., 2004) that expresses dsRed fluorescent protein in DS cells (Figure 1A), but not in the dermal papilla or interfollicular dermis. *αSMA*-expressing cells associated with the vasculature were removed by CD34 exclusion and arrector pili muscle were removed by excluding cells that express high levels of α8-integrin (ITGα8), because ITGα8 expression in DS cells is at relatively low levels (Figures 1B–1D). *αSMAdsRed*$^{+ve}$ ITGα8^{-ve} CD34^{-ve} DS cells were isolated from adult anagen (postnatal [P] 27) backskin by FACS (Figures 1C and 1D) and then grown in vitro (for 48 hr) in the presence of a GFP-expressing lentiviral vector in order to permanently label all isolated DS cells. On day 3, GFP^{+ve}*αSMAdsRed*$^{+ve}$ CD34^{-ve} DS cells were then transplanted into the "patch assay" of HF formation (Biernaskie et al., 2009; Zheng et al., 2005). After 12 days, many newly formed follicles within the grafts contained GFP^{+ve}*αSMAdsRed*$^{+ve}$ DP-derived cells, and closer inspection revealed GFP^{+ve} cells within both DS and DP compartments (Figure 1F) suggesting that prospectively isolated DS cells are capable of multilineage differentiation within the HF. Interestingly, although transplanted GFP^{+ve}*αSMAdsRed*$^{+ve}$ cells integrating into the DS of new follicles exhibited persistent *αSMAdsRed* expression, donor cells integrating into the DP compartment showed an absence of *αSMAdsRed* expression, suggesting that niche-dependent signals caused downregulation of *αSMA* expression and differentiation to a DP cell fate.

We then asked whether prospectively isolated adult *αSMAdsRed*$^{+ve}$ DS cells were capable of generating self-renewing colonies in vitro (i.e., SKPs) (Biernaskie et al., 2009; Fernandes et al., 2004). Indeed, *αSMAdsRed*$^{+ve}$ CD34^{-ve} cells were enriched 4-fold for primary SKPs formation when compared to the αSMAdsRed^{-ve} fraction (Figures 1G and 1I). Moreover, isolated DS cells exhibited serial self-renewal over two serial passages (Figures 1H and 1I), while the *αSMAdsRed*$^{-ve}$ population showed negligible colony formation (Figures 1G and 1I). Immunofluorescence analysis of tertiary *αSMAdsRed*$^{+ve}$ CD34^{-ve}-derived colonies showed that they remained mitotically active (Figure 1J) and were able to generate *Sox2*-expressing cells indicative of adult DP cells (Figure 1K). Taken together, these results suggest that prospectively isolated adult pelage DS cells generate SKPs when grown in vitro, are capable of functionally reconstituting both the DS and DP compartments of the HF and that local environmental cues influence their differentiation/phenotype. Based on these data, we hypothesized that the adult DS harbors a self-renewing dermal stem cell that functions to generate new dermal cells at the onset of each hair cycle.

Figure 1. Prospectively Isolated Dermal Sheath Cells Repopulate Both DP and DS Compartments and Self-Renew In Vitro

(A) Adult P28 *αSMAdsRed* mouse backskin showing exclusive expression within HF dermal sheath cells (red). DP is indicated by dashed lines. Note that DP cells do not express *αSMAdsRed*. Nuclei are labeled with Hoechst staining (blue).

(B) Adult P28 *αSMAdsRed* mouse backskin stained for ITGα8 (green) showing exclusive labeling of arrector pili muscle (arrowheads), with weak expression in dermal sheath (red, arrows).

(C and D) FACS plots for prospective isolation of *αSMAdsRed*$^{+ve}$ CD34^{-ve} ITGα8^{-ve} dermal sheath cells from adult P28 *αSMAdsred* mice.

(E) Schematic of patch assay of the ex vivo HF formation.

(F) Representative images of newly generated HFs within a graft after 2 weeks. Prospectively isolated dermal sheath cells (green) reconstituted the dermal sheath (arrows), as well as the DP (arrows). Note that donor sheath cells recruited to the DP, no longer express *αSMAdsRed*. n = 3 transplant experiments.

(G) Prospectively isolated *αSMAdsRed*$^{+ve}$ dermal sheath cells are enriched for SKPs formation and retain expression *αSMAdsRed* expression (red).

(H) αSMAdsRed^{+ve} cells exhibit self-renewal over three passages.

(I) Quantification of spherical colony formation over three passages. n = 2 independent experiments.

(J) Colonies generated from prospectively isolated dermal sheath cells contain Ki-67^{+ve} dividing cells (green) that are both *αSMAdsRed*$^{+ve}$ (red, arrow) and *αSMAdsRed*$^{-ve}$ (arrowhead).

(K) DS-derived self-renewing colony stained for Sox2 (green, arrowhead).

Scale bars represent 50 μm. See also Figure S1.

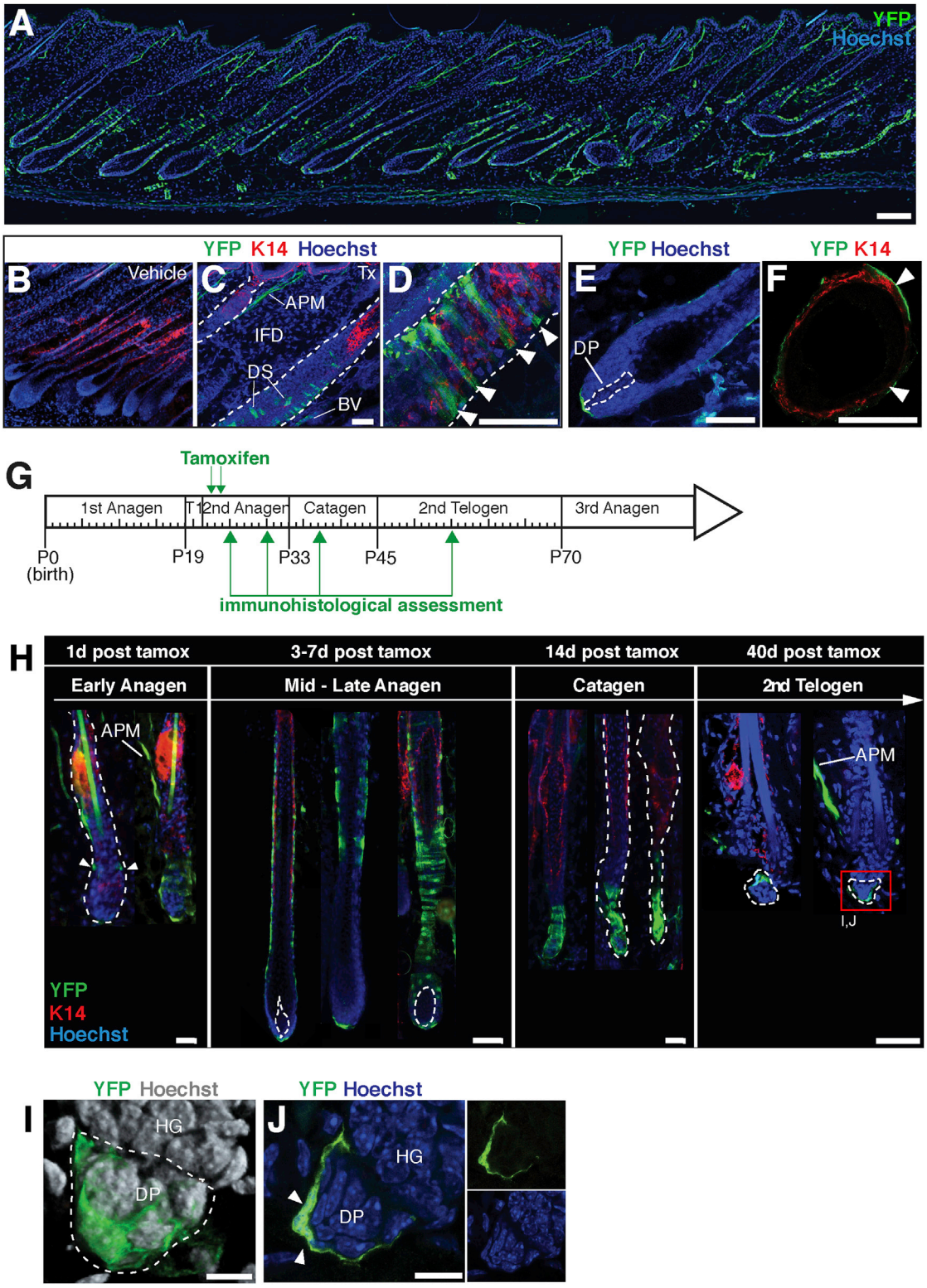

Figure 2. Hair Follicle Dermal Stem Cells Proliferate to Regenerate the Dermal Sheath and Are Retained around the Dermal Papilla over Consecutive Hair Cycles

(A) Low-magnification image of dorsal back skin 3 days following tamoxifen administration. Second anagen HFs from dorsal skin sections harvested 2–7 days after tamoxifen or vehicle (sunflower seed oil) treatment.

(B) No YFP expression is observed following oil injection. ORS keratinocytes are labeled with K14 (red).

(legend continued on next page)

The DS Contains Self-Renewing Precursors that Are Retained over Consecutive Cycles

To test this hypothesis, we performed in vivo lineage tracing experiments of DS cells within the adult mouse backskin. Tamoxifen administration to $\alpha SMACreER^{T2}:ROSA^{YFP}$ mice (referred to as $\alpha SMACreER^{T2}:YFP$) at postnatal day (P) 23/P24 (early anagen) resulted in permanent YFP expression exclusively within cells comprising the HF DS (Figures 2A, 2C, and 2D) and was observed in nearly all backskin HFs (on average 94.0%) (Figure 2A; Table S1). YFP expression was not observed prior to tamoxifen administration (Figure 2B) and although arrector pili and vasculature-associated smooth muscle cells were labeled, no $\alpha SMACreER^{T2}:YFP^{+ve}$ cells were observed in either the DP, interfollicular dermis or epithelial components of the HF (Figures 2C and 2E). YFP^{+ve} DS cells can be observed lying adjacent to K14-expressing keratinocytes of the outer root sheath (Figures 2D and 2F).

We then examined the fate of YFP^{+ve} sheath cells over the course of the first adult hair cycle (fate mapping schedule is shown in Figure 2G). Figure 2H shows multiple representative follicles from each stage of the HF cycle following tamoxifen application. One day following tamoxifen administration, a small number of YFP^{+ve} cells were observed in the early anagen DS followed by a dramatic expansion of YFP^{+ve} cells by mid/late anagen (1 week posttamoxifen). It is important to note that with this particular fate-mapping schedule, YFP-expression was limited to the DS and never observed in the second anagen DP (Figures 2E and 2H, mid-late anagen), indicative of exclusive DS expression. As the transient region of the HF degenerated during catagen (P36), YFP^{+ve} DS cells appeared to collapse around the degenerating epithelial portion of the follicle. To our surprise, as the cycle progressed to telogen, a small number of these initially labeled YFP^{+ve} cells escaped cell death and were retained around the periphery of the telogen DP (Figure 2H, second telogen, 2I, and 2J). In almost every follicle examined, YFP^{+ve} cells were retained around the telogen DP and exhibited extensive processes intercalating between DP cells (Figures 2I, 2J, and S2C). We examined >120 second telogen HFs (n = 3 mice) and found that on average, 3.4 ± 0.16 YFP^{+ve} cells were retained in each telogen follicle (ranging between 1 to 6 cells; Figure 3V). This variance is likely due to reduced penetrance in adult follicles at P23/24, but because we never observed more than six cells (even when tamoxifen dose and duration were varied), we concluded that the hair follicle dermal stem cell (hfDSC) "pool" is comprised of approximately three to six cells per follicle.

Self-Renewing Dermal Stem Cells Regenerate the DS and Contribute New Cells to the DP over Multiple Hair Cycles

To determine the longevity and fate of DS precursors over consecutive regenerative cycles, $\alpha SMACreER^{T2}:YFP$ mice were treated with tamoxifen at P23/24 and then depilated at the subsequent telogen (P45) and then monthly thereafter for three consecutive months (experimental schematic, see Figure 3A). At each subsequent anagen stage, 95.1% ± 1.6% of all backskin HFs had DS primarily comprised of YFP^{+ve} cells (third anagen: 94.6% ± 2.4%, Figures 3C and 3F; fourth anagen: 91.9% ± 3.5%, Figure 3G; fifth anagen: 98.9% ± 0.3%, Figure 3L; see also Figures S2A and S2B; Table S1) demonstrating hfDSC longevity and capacity to serially reconstitute the DS over multiple cycles.

We then asked whether hfDSCs are capable of generating functional DP cells? Despite the absence of YFP^{+ve} cells in any DP during the cycle immediately following tamoxifen application (2nd anagen), when follicles progressed to third anagen we found that 20.7% ± 2.8% of follicles contained YFP^{+ve} (sheath-derived) cells within the DP (Figures 3B, 3D, 3E, and S2A). In addition to being situated throughout the DP, YFP^{+ve} cells coexpressed the DP markers versican (Figures 3D and S3A), LEF-1 (Figure S3B), ITGα9 (Figure S3C), and noggin (Figure S3D). Because ITGα9 and LEF-1 are not expressed in the adult DS, this suggests that hfDSC progeny are recruited into the DP and adopt a phenotype consistent with native DP cells. This was further confirmed when we found YFP^{+ve} progeny in the DP also expressing Sox2 (Figure S3F). To determine whether hfDSCs replenish the DP with new cells upon each regenerative cycle, we extended the chase period over two additional hair cycles. Remarkably, in each consecutive cycle, YFP^{+ve} hfDSC progeny had repopulated the anagen DP (fourth anagen, Figures 3G–3K; fifth anagen, Figures 3M and 3N) and were observed at all depths of the DP niche.

We also asked whether the fate distribution of YFP^{+ve} hfDSC progeny changed over repeated hair cycles. The percentage of YFP^{+ve} DS cells per anagen follicle was unchanged between third and fifth cycles (Figure 3P; $p > 0.10$), suggesting that hfDSCs persist over multiple cycles and exhibit a similar reconstitution capacity with each cycle. Interestingly, we did observe a slight but significant decline at fourth anagen. This may indicate natural variations due to stochastic fate choices within each follicle. In other words, differentiation to a DP versus a DS fate may consequently impact the overall contribution to the DS, or to subsequent cycles. This is addressed below.

(C) $\alpha SMACreER^{T2}:YFP$ expression is limited to DS, arrector pili and vascular smooth muscle cells. Importantly no other cells within the HF are labeled and no intrafollicular dermal cells are labeled in normal adult skin. ORS keratinocytes are labeled with K14 (red).
(D) High-magnification image showing expression of YFP (green) in dermal sheath cells wrapping the HF. Keratin14 (red) labels ORS epithelial cells.
(E) $\alpha SMACreER^{T2}:YFP^{+ve}$ cells are not observed in the DP following tamoxifen administration. DP is outlined by dashed lines.
(F) Dorsal view of HF showing location of YFP^{+ve} cells within the dermal sheath surrounding the ORS (K14 shown in red).
(G) Experimental outline showing the HF cycle, tamoxifen administration and time course of fate mapping assessment.
(H) Representative images showing fate of $\alpha SMACreER^{T2}:YFP^{+ve}$ cells (green) at each stage of the adult HF cycle. Note that a small number of DS cells are initially labeled at the onset of anagen and these are amplified to regenerate the dermal sheath. Follicles undergo regression where sheath cells collapse around the transient portion of the follicle and subsequently are lost. Subsequently, at telogen, a small number (3–6) of $\alpha SMACreER^{T2}:YFP^{+ve}$ cells are retained around the periphery of the DP. K14 staining (red) shows ORS keratinocytes.
(I and J) Magnified images of $\alpha SMACreER^{T2}:YFP^{+ve}$ DS cells (green) surrounding the telogen DP, 40 days after tamoxifen. Note the elaborate processes contacting multiple DP cells.
APM, arrector pili muscle; BV, blood vessels; DP, dermal papilla; DS, dermal sheath; IFD, interfollicular dermis. Nuclei are labeled with Hoechst (blue). Scale bars represent 50 μm (A, C–F, and H); 10 μm (I and J). Hatched lines outline the follicle or DP. Arrowheads denote DS cells. See also Figure S2 and Table S1.

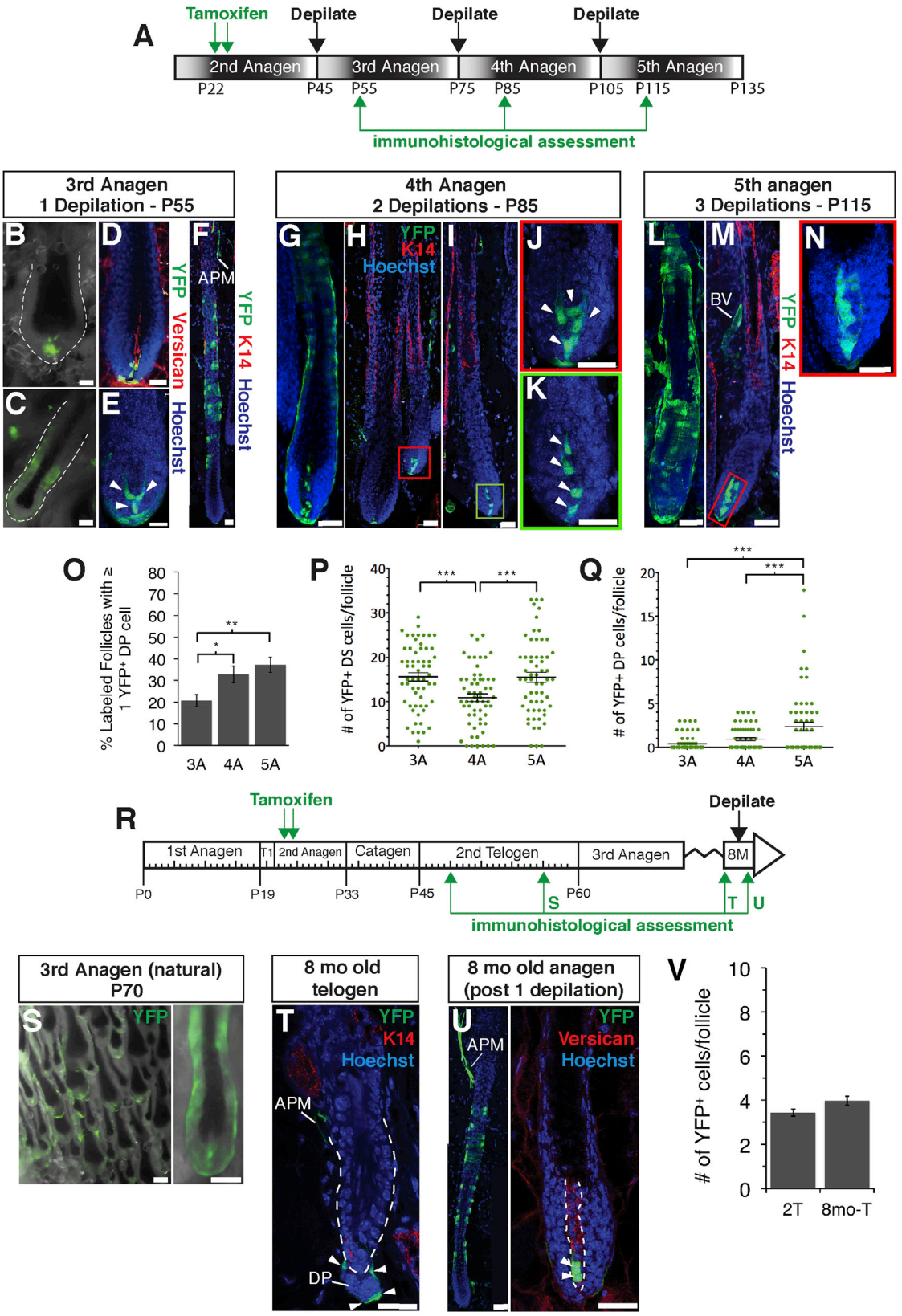

(legend on next page)

To examine DP fates, we quantified the number of follicles containing at least one YFP^{+ve} cell within the DP and found a progressive increase with each subsequent regenerative cycle from 20.7% ± 2.8% at third anagen to 32.8% ± 3.8% at fourth anagen ($p < 0.05$) and 37.3% ± 3.5% at fifth anagen cycle ($p < 0.01$) (Figure 3O). Similarly, the number of YFP^{+ve} cells recruited into each anagen DP was elevated with each subsequent hair cycle (Figure 3Q; third versus fifth anagen; fourth versus fifth anagen, both $p < 0.0001$). Taken together, these data provide strong evidence that dermal stem cells residing within the DS act as a cellular reservoir to maintain/supplement DP cell numbers with each new cycle.

In order to control for any confounding effect of repeated depilation, we performed the same DS fate-mapping experiments in naturally cycling animals (experimental schematic, Figure 3R). Animals were pulsed with tamoxifen at P23/24 and chased until 8 months of age (at which time animals would have undergone at least two additional hair cycles). Similar to our observation following depilation, hfDSCs proliferate at the onset of natural third anagen and their progeny reconstitute both DP and DS compartments (Figure 3S). We then extended the chase period for 7 months. Figure 3T (see also Figure S2D) shows a representative telogen follicle at 8 months of age (from an animal pulsed with tamoxifen at P23/24) that has undergone multiple hair cycles and retained four YFP^{+ve} hfDSCs around the periphery of the DP. Interestingly, when we quantified the average numbers of YFP^{+ve} hfDSCs per telogen follicle at P55 versus P320 (8 months of age), we found no difference (Figures 3T, 3V, S2C, and S2D) further supporting the conclusion that there is a fixed number of hfDSCs per follicle. Remarkably, anagen follicles from 8-month-old skin contained YFP^{+ve} cells in the DS (Figure 3U) and within the DP (Figure 3U).

Telogen Hair Follicle Contains Distinct DP and Sheath Compartments

Our fate mapping experiments spanning one complete adult hair cycle revealed that a subset of *αSMACreER^{T2}:YFP^{+ve}* DS cells were retained following completion of one cycle (P55) and were always observed surrounding the perimeter of the DP (Figures 2H–2J). Confocal reconstructions of YFP^{+ve} telogen follicles from second, third, and fourth hair coat showed that these YFP^{+ve} DS cells surround the DP after every cycle and remain morphologically segregated from the DP cells. Immunostaining of wild-type backskin with the DP marker estrogen receptor alpha (ERα) at anagen onset revealed that the ERα-expressing DP remains surrounded by Ki-67^{+ve} ERα^{-ve} cells (Figure S4A) and occupies the same location as the *αSMACreER^{T2}:YFP^{+ve}* cells retained over multiple cycles. At telogen, the *αSMACreER^{T2}:YFP^{+ve}* cells can be distinguished from DP cells by their unique expression of ITGα8 (Figure S2E). We then administered tamoxifen in *αSMACreER^{T2}:YFP* neonatal mice (P3/4; first anagen) and then pulsed with the thymidine analog EdU at the onset of second anagen (P20–P22). After a 6 hr chase period, YFP^{+ve} cells surrounding the DP colocalized with EdU (Figure S4B), suggesting that the cells retained in this niche are mitotically active in the subsequent cycle, whereas the DP cells do not proliferate. Taken together, these data suggest that the DS contains self-renewing cells and, despite its close proximity, remains functionally distinct from the DP at all stages of the regenerative cycle.

hfDSC Progeny Exit the DP at Catagen Either to Reintegrate into the Stem Cell Niche or to Undergo Cell Death

The lack of YFP^{+ve} hfDSC progeny within the telogen DP suggested that DP cells were actively exiting the DP during HF regression. Because, during homeostasis we do not observe YFP^{+ve} cells outside the hair follicle, we assumed that exiting DP cells would either undergo apoptosis or possibly reenter the stem cell pool. To determine the fate of hfDSC progeny within the DP after hair follicle regression, we costained adult skin for the Wnt effector LEF1 (that expressed in the nuclei of DP cells, but not in the DS or dermal cup region that is defined as the lower DS, distal to Auber's line) and ITGα8 (that specifically marks the DS and dermal cup, but not the DP). Serial imaging of hair follicles transitioning from late anagen to telogen (Figures 4A–4D) showed that YFP^{+ve} cells in the DP begin to detach, moving distally away from the LEF1^{+ve} DP aggregate. During this transition, they downregulate LEF1 expression and upregulate ITGα8, suggesting adoption of a DS fate (Figures 4B and 4C, arrows). Interestingly, as emigration proceeds, the thickness of the dermal cup increases and the appearance of an intermediate

Figure 3. *αSMACreER^{T2}:YFP^{+ve}* hfDSCs Regenerate the Dermal Sheath and Repopulate the Dermal Papilla

(A) Schematic of long-term fate mapping of dermal stem cells over multiple, consecutive (depilation-induced) hair cycles.

(B–Q) Fate of *αSMACreERT2:YFP^{+ve}* hfDSCs over four consecutive (depilation-induced) hair cycles. (B and C) Whole mount images of third anagen HFs demonstrating that YFP^{+ve} are recruited into the DP (B) and reconstitute the dermal sheath (C). (D) YFP^{+ve} cells recruited to the DP coexpress the DP marker versican (red). (E and F) Representative images showing individual YFP^{+ve} cells comprising the DP (E) and dermal sheath. (G–K) After two subsequent cycles (fourth anagen) YFP^{+ve} dermal sheath cells (green) continue to regenerate the dermal sheath (G) and also contribute cells to the DP (H–K, arrowheads). (L–N) After three subsequent cycles (fifth anagen), YFP^{+ve} dermal sheath cells (green) continue to regenerate the dermal sheath (L) and exhibit extensive recruitment to the DP (M). Magnified view of inset is shown in (N). (O) Quantification of YFP^{+ve} DS cells recruited to the anagen DP over consecutive hair cycles. n = 3 mice per time point, 600–800 anagen follicles analyzed per time point. *$p < 0.05$ and **$p < 0.005$. (P and Q) Fate distribution of YFP^{+ve} cells within anagen DS (P) and DP (Q) over repeated hair cycles. 60 anagen HFs were quantified, n = 3 mice per group. Repeated-measures ANOVA, Bonferroni post hoc ***$p < 0.0005$.

(R) Schematic of long-term fate mapping of dermal stem cells over multiple, consecutive (naturally occurring) hair cycles.

(S) Whole mount images showing third anagen HFs containing YFP^{+ve} (green) cells comprising the dermal sheath and DP.

(T) Telogen follicle from and 8-month-old mouse showing YFP^{+ve} cells (green, arrowheads) surrounding the DP.

(U) Anagen follicle from an 8-month-old mouse showing that YFP^{+ve} cells continue to regenerate the dermal sheath and are supplement cells to the DP (green, arrowheads). DP cells are stained with versican (red).

(V) Quantification of *αSMACreER^{T2}:YFP^{+ve}* cells in HFs at second telogen versus telogen at 8 months of age. n = 3 mice per time point, 20 follicles analyzed per time point. Arrector pili muscle (APM) and blood vessels (BV). Scale bars represent 25 μm.

See also Figures S3 and S4.

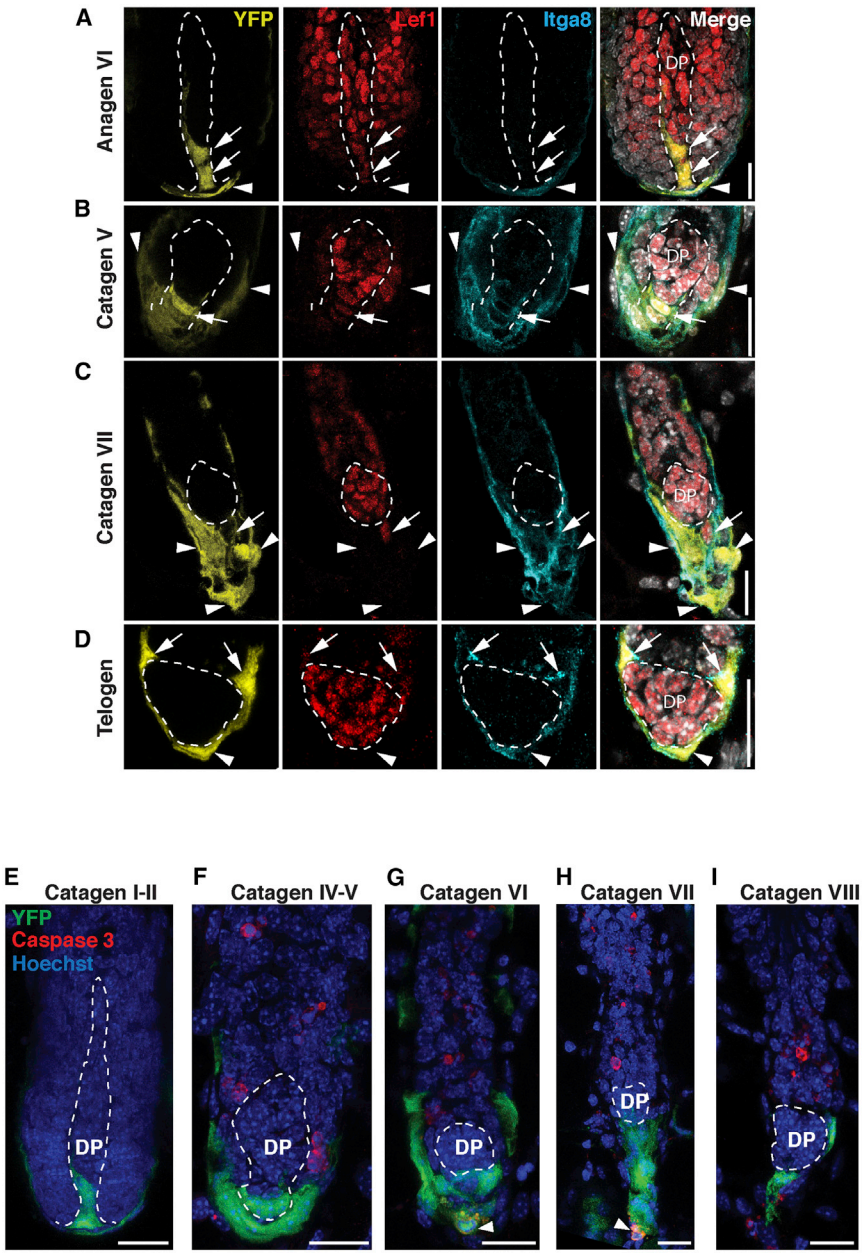

Figure 4. hfDSCs Progeny Emigrate out of the Dermal Papilla during Catagen and Reintegrate into the Dermal Cup

(A–D) Fate of *αSMACreER^{T2}:YFP^{+ve}* hfDSC progeny (yellow) in DP from late anagen to telogen. A) YFP^{+ve} cells in DP coexpress LEF1 (red, arrows), but do not express integrin-α8 (Itgα8; cyan). (B) At catagen V, YFP^{+ve} cells (yellow) have begun to move out of the DP and into the dermal cup where they exhibit a gradual downregulation of LEF1 expression (red, arrows) and begin to express Itgα8 (cyan, arrowheads). (C) At catagen VI, a single YFP^{-ve} cell has detached from the DP, but still expressing LEF1 (red) and is now positive for Itgα8 (cyan) as it transitions into the dermal cup. (D) A second telogen follicle showing YFP^{+ve} cells (yellow, arrows) that have reassembled within the hfDSC niche surrounding the DP. Coexpression of the DP marker LEF1 (red) and the DS-specific marker Itgα8 (cyan), suggests that at least some resident DP cells are retained and reintegrate into the hfDSC niche. A third YFP^{+ve} hfDSC (yellow, arrowhead) shows Itgα8 expression (cyan), but is negative for LEF1.

(E–I) Apoptotic cell death within the hair follicle mesenchyme during regression. (E) Catagen I–II, (F) Catagen IV–V, (G) Catagen VI, (H) Catagen VII, and (I) Catagen VIII shows YFP^{+ve} cells (yellow) exiting the DP do not undergo apoptotic cell death, but appear to re-integrate into the hfDSC pool. Apoptotic cell death indicated by cleaved caspase-3 (red, arrowheads) is observed in distal-most mesenchymal cells, but not in the DP, or in the intermediary cells between the DP and the distal mesenchyme.

All nuclei are stained with Hoechst (white or blue). Scale bars represent 20 μm. See also Figure S5.

population between the DP and the DS can be observed (Figures 4B, 4C, 4F, and 4G). When the follicle finally transitions into telogen, all YFP^{+ve} cells express ITGα8 and reorganize around the Lef1^{+ve} DP (Figure 4D). Interestingly, a subpopulation of YFP^{+ve} ITGα8^{+ve} cells faintly expresses Lef1 (Figure 4D, arrows) suggesting that hfDSC progeny within the anagen DP can survive catagen and reintegrate into the stem cell niche at telogen.

Previous work suggested that DP cell numbers fluctuate over the course of the hair cycle and at catagen, apoptotic cells are observed at the distal tip of the follicle bulb (Tobin et al., 2003). To determine whether emigrating YFP^{+ve} DP cells were undergoing apoptotic cell death, we stained catagen *αSMACreER^{T2}:ROSA^{YFP}* skin for cleaved caspase-3. First, we did not observe any caspase-3^{+ve} cells in the DP at any stage, consistent with previous reports (Lindner et al., 1997; Tobin et al., 2003; Weedon and Strutton, 1981). Second, YFP^{+ve} caspase-3^{+ve} mesenchymal cells were almost exclusively observed at Catagen VI–VIII in the distal-most end of the DS (Figures 4G and 4H, arrowheads). At this stage of catagen, *αSMACreERT2:YFP^{+ve}* cells had begun to vacate the DP, forming an intermediate mesenchymal layer, but we did not detect apoptotic cells within this region. Taken together, these data confirm that a subset of DP cells actively exit the DP at catagen, and although there is active apoptotic cell death within the distal DS, at least a subset of these emigrating DP cells escape cell death and reintegrate into the telogen hfDSC nice surrounding the DP.

hfDSCs Are Activated during Early Anagen

Following administration of EdU at P20–P22 (transition from telogen to anagen) we found that 81.0% ± 1.2% of YFP^{+ve} DS cells were also EdU^{+ve} (including those cells in the dermal cup) when examined at P30 (full anagen; Figures S4C and S4E, red bars). As well, on average 38.3% ± 3.0% of the YFP^{+ve} cells that were retained in each follicle following regression to second telogen

were EdU^{+ve} (P56; Figures S4D and S4E, red bars). These cells went on to generate the subsequent DS and were readily observed in the dermal cup of the subsequent third anagen follicles (Figures S4F and S4G). Notably, following two complete hair cycles post-EdU pulse, bright EdU^{+ve} cells were only observed in the dermal cup and in the DP (indicating few or no divisions), while proximal DS cells exhibited weak or no EdU signal, indicating a dilution of the label through multiple cell divisions (Figure S4F). To determine whether the YFP^{+ve} DS cells proximal to the dermal cup were a transit amplifying population, we delayed the initial EdU pulse until P24–P25. Indeed, only 38.8% ± 1.9% of YFP^{+ve} DS cells, at P30 anagen, were found to be EdU^{+ve} (Figures S4C and S4E, blue bars). At second telogen, retained YFP^{+ve} cells were only rarely EdU^{+ve} (4.9% ± 1.5% of 60 follicles) (Figures S4D and S4E) suggesting that precursors within the DS are hierarchically organized, and hfDSCs are transiently activated to proliferate and temporally coordinated following activation of epithelial bulge/secondary germ cells at the onset of anagen.

Interestingly, EdU given at P20–P22 followed by an 8 day chase resulted in a small number of DP cells that were EdU^{+ve} (Figure S4C) and similarly when extended to third anagen (Figure S4F). However, if the chase period was shortened to 6 hr, all EdU^{+ve} cells were restricted to the cells directly surrounding the DP and never found in the DP (Figure S4B), suggesting that the rare Ki67^{+ve} DP cells we observed previously (Figure S1D) were likely hfDSC progeny that had migrated into the DP compartment.

hfDSCs Are Bipotent, Replenishing Both Hair Follicle Dermal Sheath and Papilla

In order to understand whether single hfDSCs exhibit bipotency within the HF (i.e., contribution to both DS and dermal papilla compartments), we generated *αSMACreER^{T2}:ROSA^{confetti}* mice. Following the administration of tamoxifen (experimental schematic shown in Figure 5A), the confetti reporter allows stochastic expression of one of four possible fluorophores (nuclear GFP, RFP, CFP, and YFP) within Cre-expressing cells. To enhance our reporter efficiency, we generated homozygote confetti mice (*αSMACreER^{T2}:ROSA$^{confetti/confetti}$*) that generates ten different color combinations. Administration of tamoxifen at P23/24 in *αSMACreER^{T2}:ROSA$^{confetti/confetti}$* mice resulted in robust labeling of DS cells 4 days later (Figure 5B; mid anagen), with each follicle containing numerous labeled cells expressing various colors. When the chase period was extended to allow follicles to regress to second telogen (P55), 77.5% ± 4.3% of labeled follicles contained only a single fluorescent cell (hfDSC) surrounding the DP (n = 3 mice, 115 follicles; Figure 5C). Thus, the overall probability that two cells are labeled (22.5%) and that the second cell is the same color as the first (1/10 chance) is 2.2%. Based on our sample size (240 follicles total from n = 4 mice) inclusion of these relatively rare events would not be expected to significantly impact our fate analysis. Based on this, we performed fate analysis of HFs containing single color hfDSC clones in order to determine their in vivo fate potential and function. Animals were depilated to induce and synchronize HF regeneration and then follicles were examined at the middle of third anagen or at the subsequent third telogen. Out of 240 follicles examined, 78.6% ± 2.8% of clones were mitotically active, generating new cells that resided within the DS, DP, and dermal cup (the putative DSC niche) (Figures 5D–5F). To our surprise, we also observed a subset of third anagen clones (21.4% ± 0.3%) that failed to generate any progeny and remained as a single hfDSC within the dermal cup (Figure 5G). We interpreted these mitotically inactive hfDSCs to possibly represent a quiescent (reserve) population.

Our *αSMACreER^{T2}:ROSA^{YFP}* fate mapping experiments and EdU pulse-chase experiments suggested that the putative hfDSC niche in anagen follicles was in the dermal cup region. Based on this, we asked whether clones exhibited hfDSC self-renewal and expansion of the stem cell pool residing within the dermal cup. Indeed, examination of third anagen follicles in *αSMACreER^{T2}:ROSA^{confetti}* mice (240 follicles; n = 4 mice) showed that 73% of clones maintained at least one hfDSC in the dermal cup (Figure 5I) in addition to generating differentiated progeny in either DP or DS compartments. Quantification of these differentiated fates revealed that 87.4% ± 1.9% of clones generated DS cells only (Figure 5F, red clone), 7.1% ± 1.2% generated both DS and DP (Figures 5D and 5F, yellow clone), and 5.3% ± 3.0% generated only DP cells (Figure 5E). Extending the chase period to third telogen also revealed single color clones were retained around the periphery of the telogen DP (Figure 5H) (as observed in our *αSMACreER^{T2}:YFP* fate mapping experiments), consistent with a long-term repopulating hfDSC.

Interestingly, 43.9% ± 9.6% of clones exhibited an expansion of the hfDSC pool (>1 cell within the dermal cup regions), consistent with the idea that hfDSCs are capable of symmetric self-renewal (Figure 5I). Paradoxically, other hfDSC clones (19.8% ± 7.2%) had vacated the dermal cup region and had taken residence in the DS or DP (Figures S5A and S5B), suggesting that a subset of hfDSCs undergo symmetric differentiation and exit the stem cell pool. Taken together, these results support the notion that self-renewing, bipotent hfDSCs reside within the HF dermal cup and function to regenerate the DS and DP with each new hair cycle.

hfDSCs Recruitment to the DP Is Associated with Hair Type

Previous work has demonstrated that hair type is correlated with an increased number of cells within the DP (Alcaraz et al., 1993; Elliott et al., 1999; Van Scott and Ekel, 1958). In mice, ~20% of follicles that generate a zigzag hair in the primary hair coat, switch to generating a larger secondary hair type during second anagen and these larger hair types require an increased number of DP cells (Chi et al., 2013). This switching occurs with greatest frequency in the second anagen cycle. Interestingly, when we treated *αSMACreER^{T2}:YFP* neonatal pups with tamoxifen at P3/4 and examined the DP at second anagen (P28), we noticed a significant increase in recruitment of YFP^{+ve} cells into the DP (Figure 6A) relative to the degree of recruitment at later cycles (fate mapping from P3/4 to third anagen) suggesting that recruitment into the DP may be functionally linked to hair type switching. Because our fate mapping data showed that cells from the adult DS are actively recruited into the DP, we postulated that hfDSCs function to maintain/supplement cell numbers within the DP, necessary for either inductive capacity or to modulate the type of hair that is generated. To test this, tamoxifen was applied to *αSMACreER^{T2}:YFP*

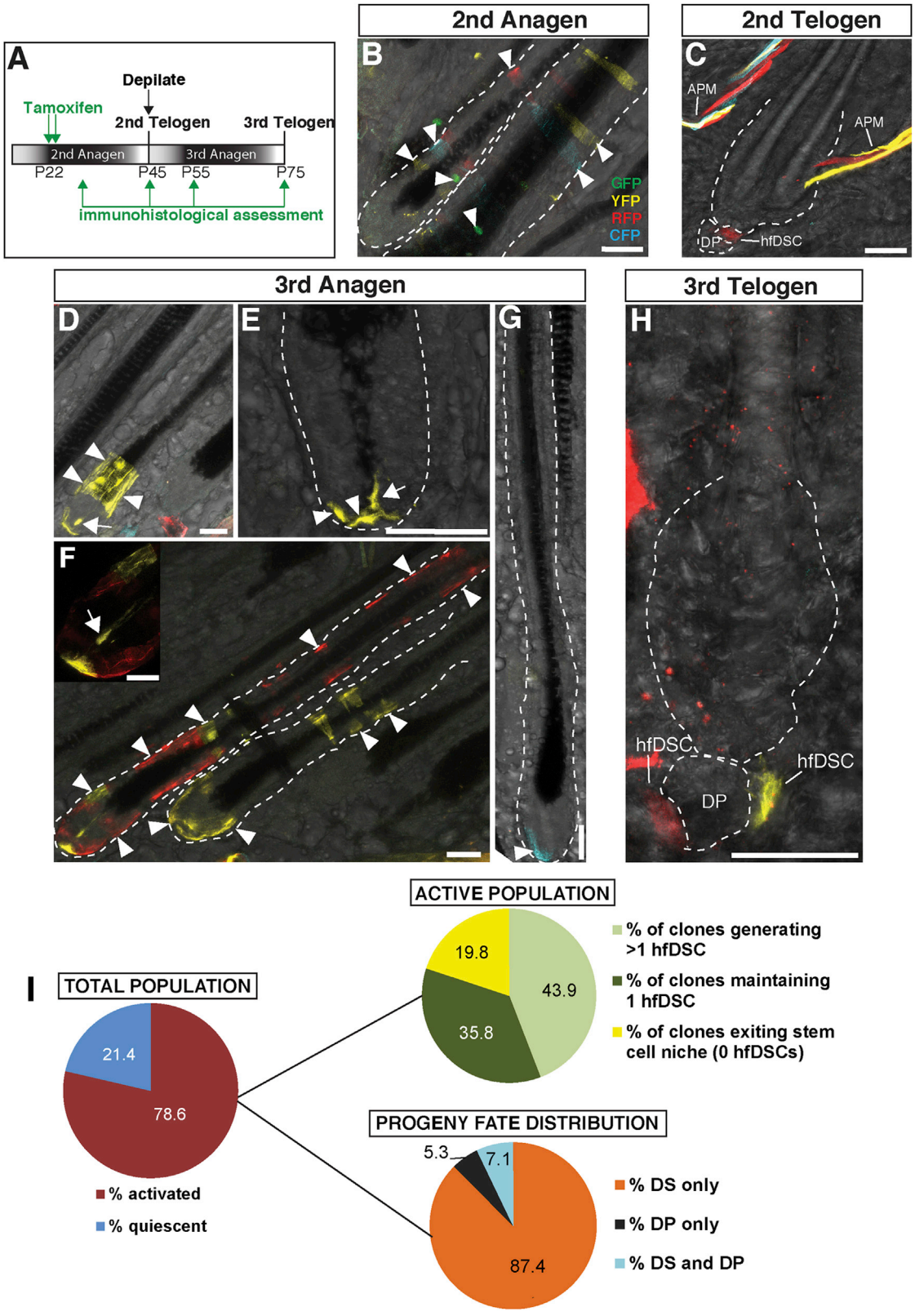

Figure 5. Clonally Identified hfDSCs Exhibit Multiple Cell Fates In Vivo

(A) Tamoxifen was administered to *αSMACreER^{T2}:ROSA^{confetti}* mice at P23–P24 and then dermal sheath cell fates were assessed at various stages of subsequent hair cycles.

(legend continued on next page)

mice at P3/4 to label hfDSC and their progeny (Figure 6B), individual backskin follicles were dissected at P28–P30 (anagen), and the frequency of YFP^{+ve} cell recruitment to the DP and the type of hair generated in both first and second hair coat for each follicle was documented. Indeed, the likelihood of YFP^{+ve} cells present within the DP was significantly elevated in follicles that had undergone a hair type switch (Figure 6F). Quantification of 300 follicles (n = 3 mice, 100 follicles from each mouse) indicated that 86.3% ± 4.1% of follicles generating a larger hair type in the second hair coat (switch from zigzag to awl/auchene) contained YFP^{+ve} cells in the DP. In contrast, follicles that did not switch (zigzag to zigzag) showed only 61.0% ± 3.0% recruitment ($p = 0.0084$; Figures 6C–6F), suggesting that recruitment of hfDSC progeny into the DP may be required to support generation of larger hair types.

Indeed, quantification of hair follicles within each revealed that hair type distribution is altered following repeated depilation; that is, small zigzag hairs were reduced in frequency and larger awl hair increased by 2-fold (Figure 6G). Interestingly, these results parallel our earlier experiments that found a persistent increase in recruitment of YFP^{+ve} sheath cells into the DP with each (depilation-induced) hair cycle (Figures 3O and 3Q). These data strongly support the idea that hfDSC progeny supplement the DP to support generation of larger hair types.

Depletion of hfDSCs Delays Anagen Onset and Alters Hair Type Specification

To test this directly, we generated mice expressing the *Diphtheria* toxin receptor (DTR) specifically within the HF DS, in order to genetically ablate hfDSCs and their progeny and then asked how this might impact HF regeneration. $\alpha SMACreER^{T2}$:$ROSA^{eYFP}$:$ROSA^{iDTR}$ mice were administered tamoxifen at P3/4 to activate expression of DTR and YFP in DS cells. Immunostaining for DTR expression in first telogen follicles shows that DTR is present in YFP^{+ve} hfDSCs (Figures S6A–S6C). To eliminate confounding effects of DTR-induced killing of αSMA-expressing cells within the vasculature, we grafted skin from adult $\alpha SMACreER^{T2}$:YFP:$iDTR^{+/-}$ and $\alpha SMACreER^{T2}$:YFP:$iDTR^{-/-}$ mice to nude mice (Figure 7A shows experimental schematic). Skin grafts were allowed to heal for 1 month (that is sufficient to allow host revascularization to occur within the graft) (Capla et al., 2006; Matsuo et al., 2007) by which time follicles had progressed to telogen. DT (*Diphtheria* toxin) was administered for 3 days prior to depilation of the graft (to synchronize hair regeneration) and continued for 7 days following in order to kill hfDSCs during the transition from telogen to anagen. Gross observation of grafts 3 weeks later revealed that DT-treated DTR$^{+/-}$ grafts exhibited a retarded entry to anagen, followed by delayed anagen progression. In contrast, PBS-treated DTR$^{+/-}$ grafts had completed anagen and progressed to catagen/telogen by 16 days (Figure 7B). Examination of YFP expression showed a marked reduction in YFP^{+ve} cells following DT treatment (Figure S6D). As well, $\alpha SMACreER^{T2}$:YFP:$iDTR^{-/-}$ grafts treated with DT exhibited similar growth to PBS-treated grafts. Quantification of hair length from hairs plucked from each condition showed that depletion of hfDSCs and/or their progeny resulted in a reduction in hair length (Figures 7C–7E) of both zigzag and awl/auchene hairs ($p < 0.01$; at both pre- and posttime points 100 hairs/graft were analyzed, n = 9 DT-treated DTR$^{+/-}$, n = 4 PBS-treated DTR$^{+/-}$ and DT-treated DTR$^{-/-}$).

Based on our finding that recruitment of hfDSC progeny is involved in supplementing new cells to the DP to support the formation of larger hair types, we asked whether depletion of hfDSCs altered the distribution of hair types generated within each graft. Analysis of 100 hairs from experimental and control grafts (n = 9 DT-treated DTR$^{+/-}$ grafts; n = 4 PBS-treated DTR$^{+/-}$ and DT-treated DTR$^{-/-}$ grafts) revealed that the frequency of each hair type was equivalent in all grafts prior to depilation ($p > 0.10$; Figures 7F and 7G). Hair depilation in control grafts resulted in a slight decline in zigzag hairs and a concomitant modest increase in awl/auchene hairs ($p > 0.10$; Figures 7F and 7G). In contrast, administration of DT at the onset of anagen actually reversed this effect. That is, depletion of hfDSCs reduced the generation of awl/auchene hairs in favor of zigzag hairs ($p = 0.02$; Figures 7F and 7G). This result further supports the conclusion that hfDSCs supplement the DP with cells to modify the inductive signaling required for normal anagen induction and hair type specification.

To determine whether this phenotype was directly related to a reduction in DP cells, we measured the total number of DP cells per follicle in DT-treated DTR$^{+/-}$ and PBS-treated DTR$^{-/-}$grafts. Quantification of follicles containing YFP^{+ve} cells confirmed there was ~23% reduction in the number of follicles that contained YFP^{+ve} cells following DT treatment (Figure 7H) and ~20% reduction in the number of DP that contained YFP^{+ve} cells (Figure 7H), suggesting a reduction in hfDSC progeny into the DP. Interestingly, however, there was no difference in the average number of DP cells per follicle (Figure 7I), most likely due to compensation from DTR^{-ve} hfDSCs, which would be expected of an active stem cell population. Taken together, genetic ablation of hfDSCs at onset of anagen results in at least a transient disruption in hair growth and altered hair phenotype.

DISCUSSION

Here, we provide direct in vivo evidence for the existence of a self-renewing dermal stem cell that resides in the HF mesenchyme. HF dermal stem cells (hfDSCs) are long-lived and

(B) Four days post-tamoxifen, mosaic expression was observed with all four fluorophores expressed throughout the dermal sheath.
(C) Following regression, telogen follicles retained one or two cells around the periphery of the DP. Representative single RFP^{+ve} cell is shown within second telogen follicle.
(D–H) Analysis of fates in the subsequent hair cycle (third anagen). Single clonal dermal stem cells exhibit bipotency, contributing to both dermal sheath and DP (D, yellow clone; F, yellow clones). (E) hfDSC generating multiple a second stem cell within the cup and one DP cell (yellow clone). (F) hfDSC clone generating DS cells only (F, red clone). (G) Quiescent hfDSC clone (cyan). (H) Two $\alpha SMACreER^{T2}$:$ROSA^{confetti}$ clones (yellow and red) observed in third telogen, demonstrating that adult hfDSCs are retained within their niche after two complete regenerative hair cycles.
(I) Frequency distributions for hfDSC behavior between second and third anagen. n = 4 mice, 240 follicles were analyzed in total. Arrector pili muscle (APM). Scale bars represent 50 μm (A–C and E–I); 25 μm (D and J).

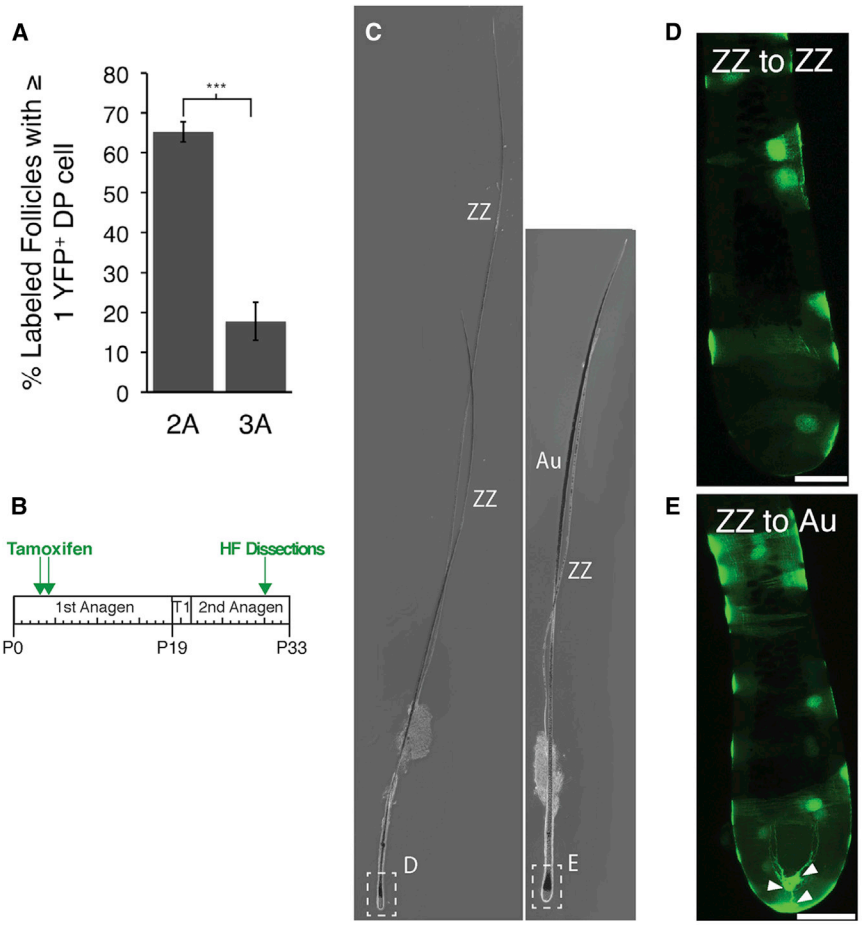

Figure 6. hfDSCs Function to Repopulate the DP and Are Required for Hair Type Specification

(A) Quantification of YFP^{+ve} cell recruitment into the DP over consecutive natural hair cycles (tamoxifen applied at P3–P4, first anagen). Second anagen showed a 3-fold increase in recruitment relative to third anagen. n = 3 mice, 400–500 follicles. ***$p < 0.0001$.

(B) Experimental schematic showing tamoxifen application in neonatal (P3–P4) *αSMACreER^{T2}:YFP* mice, followed by HF analysis at P30, following appearance of the second hair coat.

(C) Image of two (adjacent) adult second anagen HFs dissected from skin of P30 *αSMACreER^{T2}:YFP* mice that were administered tamoxifen at P3 and P4.

(D and E) Higher magnification images showing YFP^{+ve} cell fates. E) YFP^{+ve} cells were recruited into the DP of the follicle that generated a larger (auchene) secondary hair, whereas follicles that do not exhibit hair type switching (D) and generate a second small (zigzag) hair fiber do not contain newly recruited YFP^{+ve} cells.

(F) Frequency of YFP^{+ve} cell recruitment at second anagen in follicles generating similar (zigzag to zigzag) or larger (zigzag to awl/auchene) secondary hair fibers. n = 3 mice, 100 follicles from each. **$p = 0.0084$.

(G) Quantification of different hair types following repeated depilations shows a sustained increase frequency of awl hairs at the expense of zigzag hairs with each depilation. n = 3 mice, 100–200 follicles per mouse. *$p < 0.05$. Scale bar represents 50 μm.

bipotent, functioning to repopulate the DP and DS with each new regenerative cycle.

Due to the structural changes that occur during HF regeneration, the hfDSC niche is dynamic. At anagen, bipotent contribution to DP and DS coincided with residence of labeled cells in the dermal cup. This is consistent with previous work in which DS cells microdissected from distal, but not proximal regions of the HF, were able to reconstitute both DP and DS compartments ex vivo (McElwee et al., 2003). Interestingly, despite recruitment of hfDSC progeny to all proximal-distal depths of the anagen DP, at telogen YFP^{+ve} cells were only observed surrounding the periphery of the ERα^{+ve} DP. This highlights the dynamic nature of the hfDSC niche and the active cellular reorganization that occurs within it during HF regression. Indeed, during catagen, hfDSC progeny within the DP actively segregate from the DP, downregulate DP markers (LEF1), upregulate DS markers (ITGα8), and reintegrate within the hfDSC niche surrounding the telogen DP. Although there is active cell death within the DS, this seems to occur distal to cells emigrating from the DP. Overall, this suggests that some hfDSC-derived DP cells may not be entirely committed but are able to resume their hfDSC function when exposed to a permissive microenvironment (i.e., in the dermal cup). We propose that recruitment of hfDSC progeny into the DP niche may actually provide protection from the ongoing cell death that occurs outside the DP during catagen. Future experiments using a DP-specific, inducible genetic marker (that is not expressed in the dermal cup) will be required to definitively determine whether emigrating DP cells are able to reacquire bipotent hfDSC function.

hfDSCs exhibit various possible fates within a given hair cycle. Our transplantation studies showed that prospectively

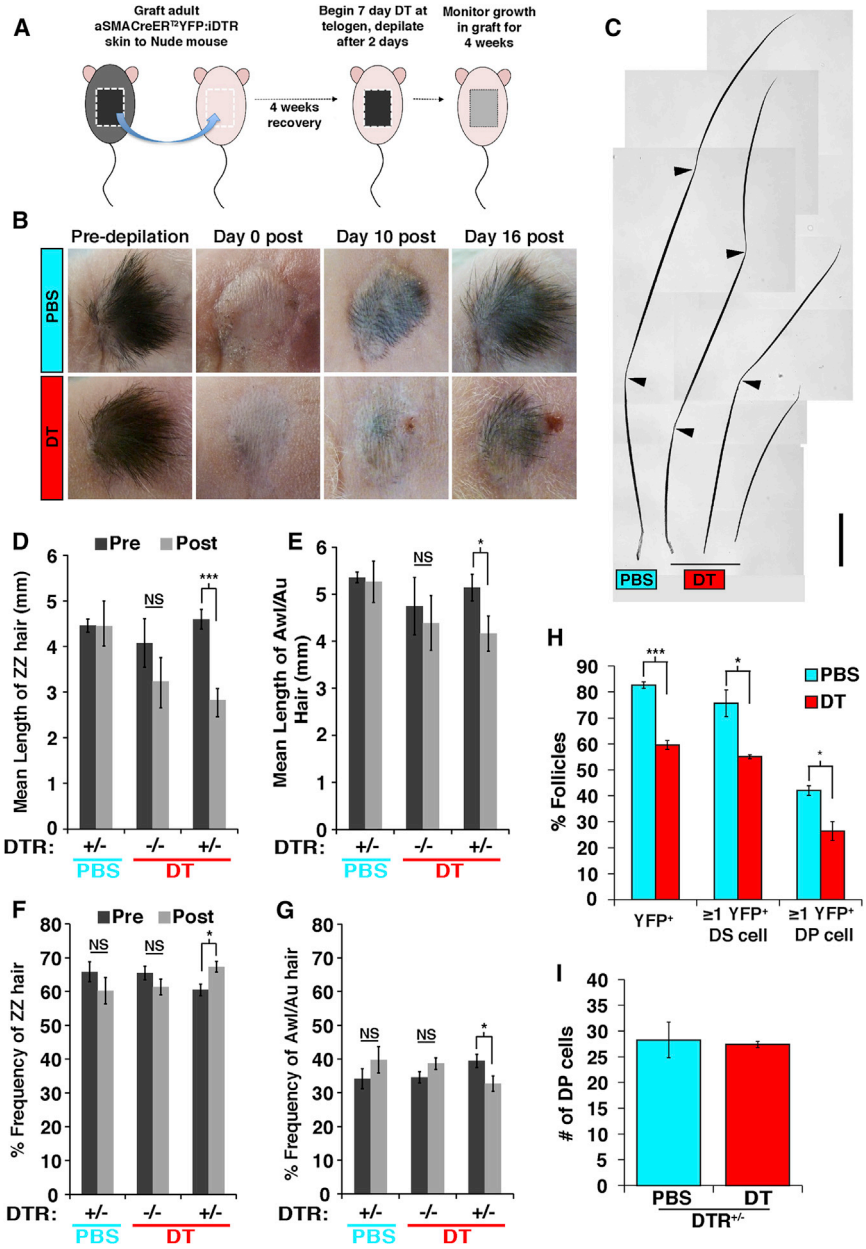

Figure 7. Depletion of hfDSCs Results in Delayed Hair Growth and Prevents Formation of Larger Hair Types

(A) Experimental schematic of hfDSC ablation within $\alpha SMACreER^{T2}:ROSA^{iDTR}$ skin grafts.

(B) $\alpha SMAcreER^{T2}:YFP:ROSA^{iDTR}$ skin grafts from mice treated with PBS or DT.

(C) Representative images of zigzag hairs plucked from PBS versus DT-treated DTR$^{+/-}$ grafts.

(D) Quantification of zigzag hair length within grafts before and after depilation-induced hair regrowth (following progression to telogen). Zigzag length was stunted following DT treatment of DTR$^{+/-}$ grafts (paired t test, p = 0.0002), but was unchanged in control groups (p = 0.97).

(E) Quantification of awl/auchene hair length (paired t test, DT-treated DTR$^{+/-}$ p = 0.01; control grafts p = 0.69). Control grafts n = 4; DT grafts n = 9; 100 hairs/graft were analyzed.

(F and G) Quantification of zigzag and awl/auchene hair frequency in grafts before and after depilation-induced hair regrowth. Control grafts resulted in a slight decrease in zigzag hairs but a modest increase in awl/auchene hair (pre versus post). DT-treatment on DTR$^{+/-}$ grafts reversed this effect, increasing zigzag hairs (pre versus post, p = 0.02) and concomitantly reducing the frequency of awl/auchene hairs (p = 0.02). Hair types frequencies did not differ between groups prior to depilation.

(H) Percent follicles containing YFP^{+ve} cells in $\alpha SMAcreER^{T2}:YFP:iDTR^{+/-}$ skin grafts treated with either PBS or DT. DT treatment reduced the frequency of YFP^{+ve} cells in the DS and in DP. Data are mean ± SEM. n = 3 grafts per group, 500 follicles counted from each graft.

(I) Quantification of total DP cell number per follicle $\alpha SMAcreER^{T2}:YFP:iDTR^{+/-}$ skin grafts following DT or PBS treatment. n = 3 grafts per group, 50 follicles per graft. Scale bar represents 500 μm. *p < 0.05, ***p < 0.0005. NS, nonsignificant.

See also Figure S6.

isolated DS cells were capable of reconstituting both DS and DP compartments. As well, they could be grown at clonal density in vitro as SKPs, over multiple passages and generated Sox2^{+ve} $\alpha SMAdsRed^{-ve}$ cells, consistent with a DP cell phenotype (Biernaskie et al., 2009; Driskell et al., 2009). Clonal fate mapping of individual (telogen stage) hfDSCs confirmed their bipotency, with single clones readily contributing cells to both DP and DS compartments. hfDSCs appeared to be biased to generating DS, which is not surprising because reconstitution of a new DS with each cycle would require the greatest number of cells. There is also a notable balance of stem cell loss (differentiation and exit from the hfDSC niche) versus expansion of the hfDSC pool. Although our data cannot definitively determine the mode of cell division that hfDSCs undertake, indirect evidence demonstrating an expansion of the hfDSC pool (43.9% of active single cell clones) suggests that hfDSCs self-renew via symmetric cell division. In parallel, depletion of the stem cell pool, exemplified by a loss of labeled clones in the hfDSC niche, would likely also occur by symmetric differentiation, which we also observed in 19.8% of active clones. Future studies using in vivo live imaging will seek to clarify this further.

Interestingly, our clonal analysis also revealed that a subset of hfDSCs within the dermal cup appear to be quiescent (mitotically inactive over the course of one hair cycle). This is in line with our long term EdU pulse chase experiments where we regularly observed a small number of EdU^{+ve} cells within the dermal cup even following two complete cycles in which most other hfDSCs have diluted the label. These data are consistent with the idea that hfDSCs are bipotent and exist as both active and quiescent stem cells, as has been described for epithelial stem cells in HF bulge and intestine (Li and Clevers, 2010).

Our lineage tracing strategy also revealed a fascinating connectivity within the DP niche, with labeled hfDSC progeny elaborating long cytoneme-like processes that extend through the depth of the DP and in some cases into the adjacent melanocyte niche. This highlights a previously unappreciated connectivity between mesenchymal compartments and identifies a physical substrate by which hfDSCs and their progeny within the DP communicate with more remote or functionally distinct regions of the DP, matrix cells and melanocytes, as opposed to local communication between neighboring cells. Indeed, a modulatory role for DP cells on melanocytes via β-catenin signaling has already been reported (Enshell-Seijffers et al., 2010). Their unique location and close proximity to DP cells (at all stages of the hair cycle) may also allow hfDSCs to act as cellular intermediate transmitting extrafollicular signals into the DP. Future studies examining the function of these morphological processes, identification of signals relayed between these connections and the molecular consequence of adding new (sheath-derived) cells to the DP will be critical toward a better understanding of the inductive process.

Although the function of the proximal dermal sheath (along the hair shaft) remains poorly understood, our data show that there are discrete functional regions within the DS, and hfDSCs can repopulate both the DS and the DP with new cells. Recent work (Chi et al., 2010) provided evidence that DP cell number is directly related to the follicle's capacity to initiate new hair growth; as DP cell numbers decline below a specific threshold, HFs are unable to initiate a new hair cycle whereas follicles retaining a sufficient number of DP remain competent to reenter growth phase. The authors suggested that the HF exploits an intrinsic mechanism to restore both DP cell number and sustain normal hair growth. Our data strongly supports this idea and show definitively that new DP cells are sourced from self-renewing, bipotent hfDSCs residing in the dermal cup.

Our results show that transient ablation of hfDSCs is sufficient to retard anagen progression and alter hair type. Our data likely underestimate the functional significance of hfDSCs to adult hair follicle regeneration. First, expression of DTR (like $\alpha SMACreER^{T2}$:$ROSA^{YFP}$) is not expressed in all telogen hfDSCs and so those escaping DT-mediated ablation ($\alpha SMACreER^{T2}$:$ROSA^{iDTR-ve}$ cells) may be able to compensate by replacing ablated cells; this is consistent with the observed delay (but not cessation) of hair follicle growth and may also explain the sustained DP cell numbers, even following DT treatment. Native DP cells are not affected by DT treatment and because we only see a small number of cells recruited to the DP with each cycle (~1–4 cells), it is not surprising that the DP remains competent to induce anagen following DT treatment. Alternatively, the impaired growth and altered hair type observed in the absence of significant DP loss could also be a consequence of impaired DS function (irrespective of any effects on the DP), because DT-mediated killing most notably impacted differentiated progeny in the DS. Future experiments will need to be done to clarify the function of the DS specifically. Last, it has been proposed that hair type specification is governed by intrinsic features of DP cells within each follicle type (Driskell et al., 2009). Although this may be the case in development, our data argue against such a mechanism in adult hair follicle regeneration and support the assertion that a putative molecular threshold within the DP may be overcome (Chi et al., 2013) or modulated by incoming hfDSC progeny. We also propose that cellular connectivity between DP cells and hfDSCs residing in the dermal cup as well as the dermal sheath may also influence matrix epithelial progenitors to alter hair type.

Related to this, a recent study reported that laser ablation of the DP renders the HF incapable of regeneration (Rompolas et al., 2012) and begs the question as to why the DP was not regenerated by hfDSCs? Because laser ablation was performed on $Lef1RFP^{+ve}$ DP cells at telogen, when hfDSCs are directly apposed to the DP and expressing Lef1, it is possible that hfDSCs were also killed with this lesion. Similarly, genetic depletion of DP cells using *Corin-Cre* (Chi et al., 2013) may also inadvertently kill hfDSCs because corin is also expressed in the hair follicle DS and dermal cup.

Future studies examining ablation of DP, at anagen or catagen, when there is greater physical separation between the DP and hfDSC compartments, will be important toward understanding the extent of hfDSC contribution to DP homeostasis and function.

In summary, we provide evidence for the existence of a dermal stem cell that resides in the hair follicle DS. Our data clarify the functional lineage relationship between the DS and the DP and demonstrates a critical role for hfDSCs in adult HF regeneration. These data also provide one of the first in vivo demonstrations of a mesenchymal stem cell contributing directly to adult tissue regeneration. Human clinical studies suggest that gradual DP cell loss and consequent dysfunction is the primary contributor to androgenetic alopecia (Randall, 2008). Our findings have direct implications toward understanding the pathological mechanisms that underlie such hair loss and identify an endogenous source of cells that may be targeted to restore DP numbers and reverse hair follicle growth arrest.

EXPERIMENTAL PROCEDURES

In Vivo Lineage Tracing

Fate mapping of adult HF DS cells was achieved by crossing $\alpha SMACreER^{T2}$ mice (Wendling et al., 2009) with a $ROSA^{eYFP}$ reporter strain or to the *Brainbow 2.0* strain ("confetti"; both from Jackson Laboratories). Tamoxifen (4-OHT; Toronto Research Chemicals) was administered by intraperitoneal injection (1 mg/20 g) or topical application to backskin (5 μl of 100 mg/ml in DMSO) twice daily on either postnatal day (P) 3 and 4 or at 23 and 24 (early anagen). EdU (5-ethynyl-2′-deoxyuridine) was administered at 100 μg/mouse. For quantification of $\alpha SMACreER^{T2}$:$ROSA^{YFP+ve}$ DS cell proliferation and recruitment into the DP, 200 follicles were analyzed per mouse (n = 3–6 mice per time point). All animal experiments received prior approval of the University of Calgary Health Sciences Animal Care Committee and were in accordance with guidelines set by the Canadian Council on Animal Care.

Dermal Stem Cell Ablation Experiments

$\alpha SMACreER^{T2}$ mice were crossed to $ROSA^{eYFP}$ and $ROSA^{iDTR}$ mice (Jackson Laboratories). At P3 and P4, pups were given topical application of tamoxifen (as above) to induce expression of YFP and DTR in backskin HF DS cells. To avoid any confounding effects of killing vasculature-associated αSMA-expressing cells, we grafted skin from $\alpha SMACreER^{T2}$:YFP:$iDTR^{+/-}$ and $\alpha SMACreER^{T2}$:YFP:$iDTR^{-/-}$ mice onto adult male Nude mice. Skin grafts were allowed to heal for 1 month, to allow host revascularization to occur within the graft (Capla et al., 2006; Matsuo et al., 2007). *Diphtheria* toxin (DT; 25 ng/g body weight, Sigma Aldrich) was administered for 3 days, prior to depilation (to synchronize hair regeneration) of the graft and continued for 7 days following in order to kill DTR-expressing hfDSCs during the transition from telogen to anagen. Control grafts received either PBS injections ($DTR^{+/-}$) or DT injections ($DTR^{-/-}$). HF regeneration was documented at 0, 10, and 16 days postdepilation and then hair fiber length and hair type was quantified from

plucked hairs (100 hairs/graft, n = 4 controls grafts, n = 9 DT-treated DTR$^{+/-}$ grafts). Hair length was measured using ImageJ software (NIH).

Immunofluorescence Staining

Antibodies are listed in the Supplemental Experimental Procedures. Skin samples were either fresh frozen, fixed for 4 hr in 4% paraformaldehyde at 4°C, or 48 hr in 2% paraformaldehyde at 4°C followed by 24 hr in 20% sucrose and subsequently snap frozen in OCT (Sakura). Image collection and quantification was done using a Leica SP8 spectral confocal microscope.

Cell Sorting and Cell Culture

Back skin from adult (P26–P28) *Sox2EGFP* mice (Ellis et al., 2004) or *αSMAdsRed* mice (Magness et al., 2004) were dissociated to single cells and sorted on a FACSAria III (Becton Dickinson) with viable cells identified by Sytox blue or red (Invitrogen). DP cells were characterized as *Sox2:GFP*$^{+ve}$ ITGα9^{+ve} to exclude *Sox2*-expressing glia cells residing in nerve terminals (Biernaskie et al., 2009; Clavel et al., 2012). DS cells were characterized as *αSMAdsRed*$^{+ve}$ and then stained for anti-CD34 and anti-ITGα8, to negatively select for interfollicular dermal cells, arrector pili muscle cells, respectively. Gates were set according to single stained positive and negative (isotype) controls. Cells were plated at 10,000 cells/ml and grown as previously described (Biernaskie et al., 2009).

Statistical Analysis

All data are represented as mean ± SEM. Data were analyzed using GraphPad Prism 6 Software using two-tailed t tests or Kruskal Wallis for nonparametric data sets. Repeated-measures ANOVA was used to examine the effect of repeated depilation on YFP^{+ve} DP and DS cell kinetics. Paired t tests were used for within graft comparisons of hair type and length before and after DT-mediated depletion. $p < 0.05$ was considered significant.

SUPPLEMENTAL INFORMATION

Supplemental Information includes Supplemental Experimental Procedures, six figures, and one table and can be found with this article online at http://dx.doi.org/10.1016/j.devcel.2014.10.022.

AUTHOR CONTRIBUTIONS

W.R. performed all lineage tracing, imaging, quantification, statistical analyses, figure preparation, and co-wrote the manuscript. S.A. and A.H. contributed equally. S.A. performed cell depletion and hair type analysis. A.H. performed proliferation kinetics experiments and in vitro analysis. E.R. generated lentiviral vectors and performed FACS. R.K. performed cell culture experiments and lentiviral transduction experiments. A.H. provided lentiviral constructs and advice. S.M. provided *αSMA*^{dsRed} mice. D.M. provided αSMACreER^{T2} mice. J.B. was responsible for conception, experimental design, and experimental supervision and co-wrote the manuscript.

ACKNOWLEDGMENTS

We thank Min Cheng, Morgan Stykel, and Sarthak Sinha for technical assistance and Molly Chisholm and Martha Hurtatis for outstanding animal care. W.R. was supported by the AIHS MD-PhD and ACHRI/CIHR studentships and SA received a UCVM Dean's Excellence Award. J.B. is a CIHR New Investigator and this work was funded by a CIHR operating grant (MOP 106646) to J.B., a Stem Cell Network Global Impact Grant, and the Calgary Firefighters Burn Treatment Society.

Received: March 3, 2014
Revised: September 24, 2014
Accepted: October 29, 2014
Published: November 26, 2014

REFERENCES

Alcaraz, M.V., Villena, A., and Pérez de Vargas, I. (1993). Quantitative study of the human hair follicle in normal scalp and androgenetic alopecia. J. Cutan. Pathol. *20*, 344–349.

Biernaskie, J., Paris, M., Morozova, O., Fagan, B.M., Marra, M., Pevny, L., and Miller, F.D. (2009). SKPs derive from hair follicle precursors and exhibit properties of adult dermal stem cells. Cell Stem Cell *5*, 610–623.

Blanpain, C., Lowry, W.E., Geoghegan, A., Polak, L., and Fuchs, E. (2004). Self-renewal, multipotency, and the existence of two cell populations within an epithelial stem cell niche. Cell *118*, 635–648.

Capla, J.M., Ceradini, D.J., Tepper, O.M., Callaghan, M.J., Bhatt, K.A., Galiano, R.D., Levine, J.P., and Gurtner, G.C. (2006). Skin graft vascularization involves precisely regulated regression and replacement of endothelial cells through both angiogenesis and vasculogenesis. Plast. Reconstr. Surg. *117*, 836–844.

Chi, W.Y., Enshell-Seijffers, D., and Morgan, B.A. (2010). De novo production of dermal papilla cells during the anagen phase of the hair cycle. J. Invest. Dermatol. *130*, 2664–2666.

Chi, W., Wu, E., and Morgan, B.A. (2013). Dermal papilla cell number specifies hair size, shape and cycling and its reduction causes follicular decline. Development *140*, 1676–1683.

Clavel, C., Grisanti, L., Zemla, R., Rezza, A., Barros, R., Sennett, R., Mazloom, A.R., Chung, C.Y., Cai, X., Cai, C.L., et al. (2012). Sox2 in the dermal papilla niche controls hair growth by fine-tuning BMP signaling in differentiating hair shaft progenitors. Dev. Cell *23*, 981–994.

Cotsarelis, G., Sun, T.T., and Lavker, R.M. (1990). Label-retaining cells reside in the bulge area of pilosebaceous unit: implications for follicular stem cells, hair cycle, and skin carcinogenesis. Cell *61*, 1329–1337.

Driskell, R.R., Giangreco, A., Jensen, K.B., Mulder, K.W., and Watt, F.M. (2009). Sox2-positive dermal papilla cells specify hair follicle type in mammalian epidermis. Development *136*, 2815–2823.

Elliott, K., Stephenson, T.J., and Messenger, A.G. (1999). Differences in hair follicle dermal papilla volume are due to extracellular matrix volume and cell number: implications for the control of hair follicle size and androgen responses. J. Invest. Dermatol. *113*, 873–877.

Ellis, P., Fagan, B.M., Magness, S.T., Hutton, S., Taranova, O., Hayashi, S., McMahon, A., Rao, M., and Pevny, L. (2004). SOX2, a persistent marker for multipotential neural stem cells derived from embryonic stem cells, the embryo or the adult. Dev. Neurosci. *26*, 148–165.

Enshell-Seijffers, D., Lindon, C., Wu, E., Taketo, M.M., and Morgan, B.A. (2010). Beta-catenin activity in the dermal papilla of the hair follicle regulates pigment-type switching. Proc. Natl. Acad. Sci. USA *107*, 21564–21569.

Fernandes, K.J.L., McKenzie, I.A., Mill, P., Smith, K.M., Akhavan, M., Barnabé-Heider, F., Biernaskie, J., Junek, A., Kobayashi, N.R., Toma, J.G., et al. (2004). A dermal niche for multipotent adult skin-derived precursor cells. Nat. Cell Biol. *6*, 1082–1093.

Jahoda, C.A. (2003). Cell movement in the hair follicle dermis - more than a two-way street? J. Invest. Dermatol. *121*, ix–xi.

Jahoda, C.A., Horne, K.A., and Oliver, R.F. (1984). Induction of hair growth by implantation of cultured dermal papilla cells. Nature *311*, 560–562.

Jahoda, C.A., Reynolds, A.J., Chaponnier, C., Forester, J.C., and Gabbiani, G. (1991). Smooth muscle alpha-actin is a marker for hair follicle dermis in vivo and in vitro. J. Cell Sci. *99*, 627–636.

Li, L., and Clevers, H. (2010). Coexistence of quiescent and active adult stem cells in mammals. Science *327*, 542–545.

Lindner, G., Botchkarev, V.A., Botchkareva, N.V., Ling, G., van der Veen, C., and Paus, R. (1997). Analysis of apoptosis during hair follicle regression (catagen). Am. J. Pathol. *151*, 1601–1617.

Magness, S.T., Bataller, R., Yang, L., and Brenner, D.A. (2004). A dual reporter gene transgenic mouse demonstrates heterogeneity in hepatic fibrogenic cell populations. Hepatology *40*, 1151–1159.

Matsuo, S., Kurisaki, A., Sugino, H., Hashimoto, I., and Nakanishi, H. (2007). Analysis of skin graft survival using green fluorescent protein transgenic mice. J. Med. Investig. *54*, 267–275.

McElwee, K.J., Kissling, S., Wenzel, E., Huth, A., and Hoffmann, R. (2003). Cultured peribulbar dermal sheath cells can induce hair follicle development and contribute to the dermal sheath and dermal papilla. J. Invest. Dermatol. *121*, 1267–1275.

Randall, V.A. (2008). Androgens and hair growth. Dermatol. Ther. *21*, 314–328.

Rompolas, P., Deschene, E.R., Zito, G., Gonzalez, D.G., Saotome, I., Haberman, A.M., and Greco, V. (2012). Live imaging of stem cell and progeny behaviour in physiological hair-follicle regeneration. Nature *487*, 496–499.

Tobin, D.J., Gunin, A., Magerl, M., Handijski, B., and Paus, R. (2003). Plasticity and cytokinetic dynamics of the hair follicle mesenchyme: implications for hair growth control. J. Invest. Dermatol. *120*, 895–904.

Van Scott, E.J., and Ekel, T.M. (1958). Geometric relationships between the matrix of the hair bulb and its dermal papilla in normal and alopecic scalp. J. Invest. Dermatol. *31*, 281–287.

Weedon, D., and Strutton, G. (1981). Apoptosis as the mechanism of the involution of hair follicles in catagen transformation. Acta Derm. Venereol. *61*, 335–339.

Wendling, O., Bornert, J.M., Chambon, P., and Metzger, D. (2009). Efficient temporally-controlled targeted mutagenesis in smooth muscle cells of the adult mouse. Genesis *47*, 14–18.

Zheng, Y., Du, X., Wang, W., Boucher, M., Parimoo, S., and Stenn, K. (2005). Organogenesis from dissociated cells: generation of mature cycling hair follicles from skin-derived cells. J. Invest. Dermatol. *124*, 867–876.